Since January 2020 Elsevier has created a COVID-19 resource centre with free information in English and Mandarin on the novel coronavirus COVID-19. The COVID-19 resource centre is hosted on Elsevier Connect, the company's public news and information website.

Gastroenterology 2020;159:1015–1018

BASIC AND TRANSLATIONAL—PANCREAS

Mortality From Coronavirus Disease 2019 Increases With Unsaturated Fat and May Be Reduced by Early Calcium and Albumin Supplementation

Bara El-Kurdi,[1,*] **Biswajit Khatua**,[2,*] Christopher Rood,[3] Christine Snozek,[4] Rodrigo Cartin-Ceba,[2] and Vijay P. Singh,[2] on behalf of the Lipotoxicity in COVID-19 Study Group

[1]Department of Medicine, East Tennessee State University, Johnson City, Tennessee; [2]Department of Medicine, Mayo Clinic, Scottsdale, Arizona; [3]Saint Louis University School of Medicine, Saint Louis, Missouri; and [4]Department of Laboratory Medicine and Pathology, Mayo Clinic, Scottsdale, Arizona

See editorial on page 824.

Keywords: Unsaturated; Fatty Acid; Coronavirus; Lipotoxicity.

Although most coronavirus disease 2019 (COVID-19) infections are self-limited, some develop into sepsis and multisystem organ failure (MSOF),[1] resembling lipotoxic acute pancreatitis.[2,3] Understanding underlying mechanisms may guide supportive care while clinical trials are ongoing. Unsaturated fatty acids (UFAs) generated by adipose lipolysis[2,3] cause MSOF, including acute lung injury.[2] Severe acute pancreatitis and severe COVID-19 share obesity as a risk factor,[4] along with lipase elevation,[5] hypoalbuminemia,[1] and hypocalcemia.[6] The latter 2 may progress undetected because calcium-albumin correction calculations (eg, https://www.mdcalc.com/calcium-correction-hypoalbuminemia) can pseudonormalize calcium values (eg, uncorrected calcium of 5.9 mg/dL and albumin of 0.1 g/dL to corrected calcium of 9.0 mg/dL). Notably, calcium ameliorates MSOF,[7] and UFAs cause nonendocrine hypocalcemia.[7]

The ACE2 receptor resides on adipocytes[8] containing triglycerides and adipocyte triglyceride lipase (ATGL) and on pancreatic acini expressing pancreatic triglyceride lipase (PNLIP).[2] Both oleic acid (C18:1) administration and adipose lipolysis[3] by PNLIP can cause acute lung injury and MSOF. These, and previous data showing that UFAs depolarize mitochondria,[2] inhibit complexes I and V,[3] decrease adenosine triphosphate, release intracellular calcium,[3] and increase inflammatory mediators,[3] made us explore lipotoxicity during severe COVID-19. This approach, culminating in clinical advice to keep calcium and albumin levels normal from early on in the disease, is summarized in Figure 1*A* and explained diagrammatically in supplementary figure 1.

Methods

See Supplementary Materials.

Results

Hypocalcemia and Hypoalbuminemia Occur Early During Severe Coronavirus Disease 2019

Seven of 15 hospitalized patients were discharged home by 3. 4 ±1.6 days. One died of hypoxemic failure after declining intubation. Seven patients with severe disease required intensive care (mean, 3.9 ± 2 days after admission). Although otherwise similar to those with mild disease, severely ill patients had higher blood urea nitrogen (BUN) level; lower platelets and lymphocytes (Supplementary Figure 2); early, steady progressive hypocalcemia and hypoalbuminemia; and lower oxygen saturation nadirs (Figure 1*B*). Mice administered linoleic acid (LA) (C18:2) (Supplementary Figure 3*A*) but not the saturated fatty acid C16:0 developed hypoalbuminemia. Because albumin and calcium bind fatty acids and reduce toxicity,[7] we graphed serum unbound fatty acids in patients in the intensive care unit (Figure 1*C*) vs their P/F ratio (ie, the arterial partial pressure of oxygen/percentage of oxygen). Lower P/F ratios (0.97 ± 0.1) were associated with higher unbound fatty acid levels (15.5 ± 7.7 μmol/L vs 4.2 ± 2.3 μmol/L; $P < .002$), and vice versa (2.36 ± 0.4; $P < .003$).

Unsaturated Fatty Acids Cause Multisystem Organ Failure and Inflammation Resembling Severe Coronavirus Disease 2019

C18:1, C18:2, and C16:0 make up 10%–50% of dietary fat and adipose triglycerides in humans. Mice given C18:1 (not shown) or C18:2, but not C16:0, (Figure 1*D*) developed leucopenia, lymphopenia,[1] lymphocytic injury, relative thrombocytopenia,[1] hypercytokinemia,[1] elevated alanine aminotransferase levels,[1] hypoalbuminemia[1], hypocalcemia[6], shock,[1] and renal failure resembling lethal COVID-19.

*Authors share co-first authorship.

Abbreviations used in this paper: ATGL, adipocyte triglyceride lipase; BUN, blood urea nitrogen; COVID-19, coronavirus disease 2019; LA, linoleic acid; LLP, 1,2-dilinoleoyl-3-palmitoyl-racglycerol; MSOF, multisystem organ failure; PNLIP, pancreatic triglyceride lipase; UFA, unsaturated fatty acid.

Most current article

0016-5085
https://doi.org/10.1053/j.gastro.2020.05.057

Mortality From Coronavirus Disease 2019 Correlates With Dietary Unsaturated Fat Intake; Saturated Fat Is Protective

Because adipose triglyceride composition corresponds to dietary fat composition, we compared dietary fat patterns to other risk factors for COVID-19 mortality from countries with >1000 COVID-19 cases reported between March 25, 2020, and April 8, 2020 (61 countries; 1,476,418 patients).

We first did a univariate analysis using the linear mixed model, accounting for daily reported percent mortality vs dietary and other factors (Figure 1*E*). Because of skewness, log-transformed mortality was used in the model. Only saturated fat intake (kg/capita/y) was negatively associated ($P = .05$), and percent UFA intake was positively associated ($P < .001$) with mortality (Figure 1*F* and *G*). The rate ratio indicates the relative change in mortality for each parameter; for example, a rate ratio of 0.97 for saturated fat intake indicates that for a 1-unit increase in saturated fat, there is a 3% reduction in mortality: (1 – 0.97) × 100% = 3%. Multivariate analysis showed only percent UFA as significantly associated with mortality ($P < .0001$).

Interestingly, per capita GDP consistently and positively correlated with tests/million (not shown), and COVID-19 cases/million (Supplementary Figure 3*B*), with the inflection point noted above US$10,000. Thus, COVID-19 may be undiagnosed in low-income countries.

We next studied how dietary and adipose triglyceride saturation could protect from severe COVID-19.

Saturated Fatty Acids in Triglycerides Impede Interaction With Adipocyte Triglyceride Lipase

Because it is not known which lipase is active in COVID-19, we examined how saturation affects triglyceride interaction with ATGL. On unbiased in silico docking simulation, the linoleic acid triglyceride trilinolein (LLL) docked to the ATGL homology model with a GlideScore of –6.71 kcal/mol and 7.02 Å between the catalytic Ser47 hydroxyl and the carbonyl C atom of the glycerol backbone (Figure 1*H*). Substituting palmitate at Sn-3, 1,2-dilinoleoyl-3-palmitoyl-racglycerol (LLP) docked with a GlideScore of –3.34 kcal/mol and 8.49 Å from the catalytic serine (Figure 1*I*). Thus, saturation reduces lipolysis by making the complex less energetically and structurally favorable.

Unsaturated Fatty Acids Injure and Impede Cell Functions; Albumin Binding Prevents but Does Not Reverse Injury

Exposure of an established human umbilical vein endothelial cell (HUV-EC-C) cell monolayer to UFAs decreased transendothelial resistance and increased dextran permeability and apoptotic peripheral blood mononuclear cells (Figure 1*J–L*). LA increased the baseline and frequency of cytosolic calcium elevation in spontaneously beating cardiomyocytes (Figure 1*M*). Thus, UFAs may cause vascular (albumin) leak, inflammatory injury, and arrhythmia during severe COVID-19.

On isothermal titration calorimetry, albumin-bound LA strongly (stoichiometry ≈ 6:1; enthalpy, –230 KJ/mol) (Figure 1*N*). However, adding albumin 30 minutes after LA to macrophages did not reduce necrosis. Although preincubating HEK293 cells with albumin and calcium (Figure 1 *O* and *P*) completely prevented necrosis, delayed addition of albumin only partially blocked or reversed LA-induced mitochondrial depolarization[2] (Figure 1*Q* and *R*). Therefore, early neutralization of UFAs may prevent mitochondrial dysfunction and injury resulting in MSOF.[3] In vivo, prophylactic calcium and albumin prevented LA-induced MSOF (not shown). Thus, early supplementation with albumin and calcium may be better than correcting deficiencies later during severe COVID-19 infection or sepsis, which may be too little, too late.

WHAT YOU NEED TO KNOW

BACKGROUND AND CONTEXT

While most COVID-19 patients clear the infection, some develop severe disease with organ failure. Based on patterns associated with severe COVID-19, underlying mechanisms, we propose a simple, low risk supportive intervention.

NEW FINDINGS

Unsaturated fat intake is associated with increased mortality from COVID-19. Unsaturated fatty acids cause injury, organ failure resembling COVID-19. Early albumin and calcium can bind unsaturated fatty acids, reduce injury.

LIMITATIONS

We do not have a clinical trial to support that "keeping a normal serum calcium and albumin all through COVID-19" improved mortality. Such a trial may be helpful in the future.

IMPACT

Both calcium and albumin are inexpensive, and easily available. If supplemented early during COVID-19 hospitalization, these may reduce organ failure and ICU requirements despite a lack of proven anti-viral therapies.

Discussion

Calcium binds C18:2 more weakly[7] (–20 kJ/mol) than albumin. However, calcium's total concentration (2.25–2.75 mmol/L) is 3–5 times higher, and it ameliorates MSOF.[7] Thus, supplementing calcium (eg, oral calcium carbonate) and albumin to normal values early during COVID-19[6] could reduce lipotoxic MSOF without violating the calcium-albumin correction. Despite COVID-19 being underdiagnosed in lower-income countries, mortality in diagnosed COVID-19 is likely from the infection and, thus, supports our conclusions. Additionally, while we did incorporate the number of ventilators per country, the numbers quoted are in some cases more than 8 years old, and therefore may not be reliable. Similarly, the number of ICU beds available may not reflect the exact number in each country. Although our clinical study is small and retrospective and experimental studies are correlative, their congruence to severe COVID-19 is supported by larger published studies[1,6] and can be validated by future interventional studies. Thus, keeping calcium and albumin levels

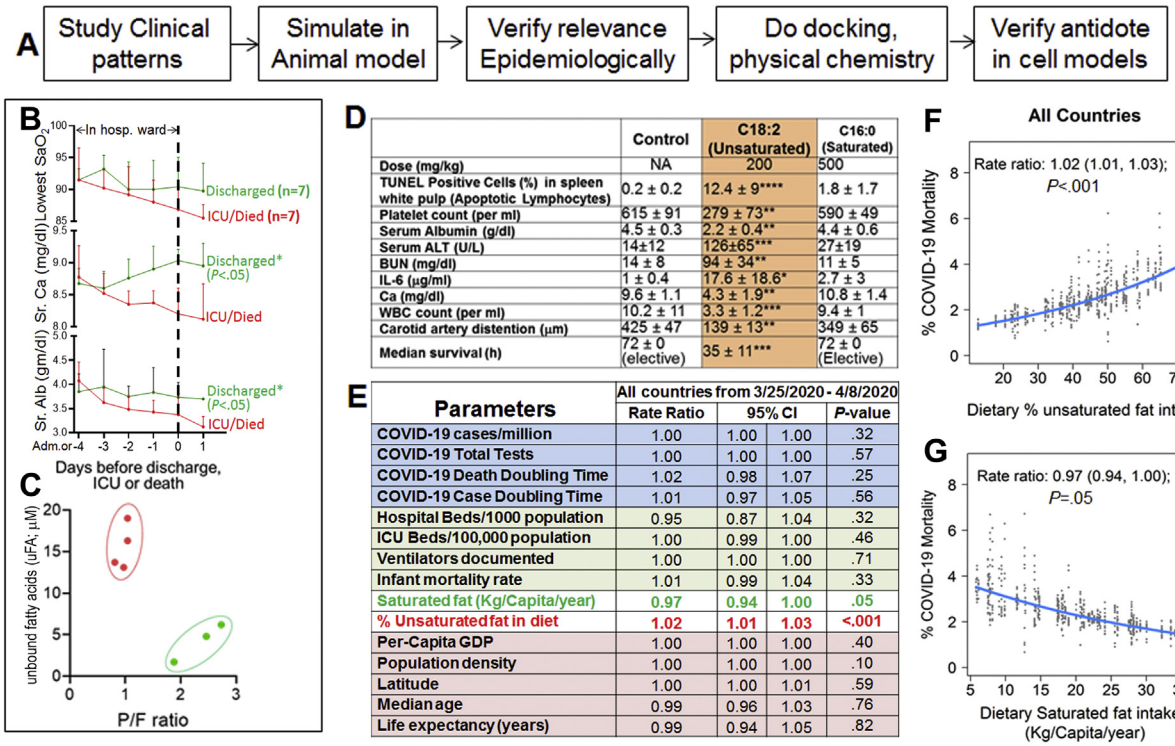

	Control	C18:2 (Unsaturated)	C16:0 (Saturated)
Dose (mg/kg)	NA	200	500
TUNEL Positive Cells (%) in spleen white pulp (Apoptotic Lymphocytes)	0.2 ± 0.2	12.4 ± 9****	1.8 ± 1.7
Platelet count (per ml)	615 ± 91	279 ± 73**	590 ± 49
Serum Albumin (g/dl)	4.5 ± 0.3	2.2 ± 0.4**	4.4 ± 0.6
Serum ALT (U/L)	14±12	126±65***	27±19
BUN (mg/dl)	14 ± 8	94 ± 34**	11 ± 5
IL-6 (µg/ml)	1 ± 0.4	17.6 ± 18.6*	2.7 ± 3
Ca (mg/dl)	9.6 ± 1.1	4.3 ± 1.9**	10.8 ± 1.4
WBC count (per ml)	10.2 ± 11	3.3 ± 1.2***	9.4 ± 1
Carotid artery distention (µm)	425 ± 47	139 ± 13**	349 ± 65
Median survival (h)	72 ± 0 (elective)	35 ± 11***	72 ± 0 (Elective)

Parameters	All countries from 3/25/2020 - 4/8/2020			
	Rate Ratio	95% CI		*P*-value
COVID-19 cases/million	1.00	1.00	1.00	.32
COVID-19 Total Tests	1.00	1.00	1.00	.57
COVID-19 Death Doubling Time	1.02	0.98	1.07	.25
COVID-19 Case Doubling Time	1.01	0.97	1.05	.56
Hospital Beds/1000 population	0.95	0.87	1.04	.32
ICU Beds/100,000 population	1.00	0.99	1.00	.46
Ventilators documented	1.00	1.00	1.00	.71
Infant mortality rate	1.01	0.99	1.04	.33
Saturated fat (Kg/Capita/year)	0.97	0.94	1.00	.05
% Unsaturated fat in diet	1.02	1.01	1.03	<.001
Per-Capita GDP	1.00	1.00	1.00	.40
Population density	1.00	1.00	1.00	.10
Latitude	1.00	1.00	1.01	.59
Median age	0.99	0.96	1.03	.76
Life expectancy (years)	0.99	0.94	1.05	.82

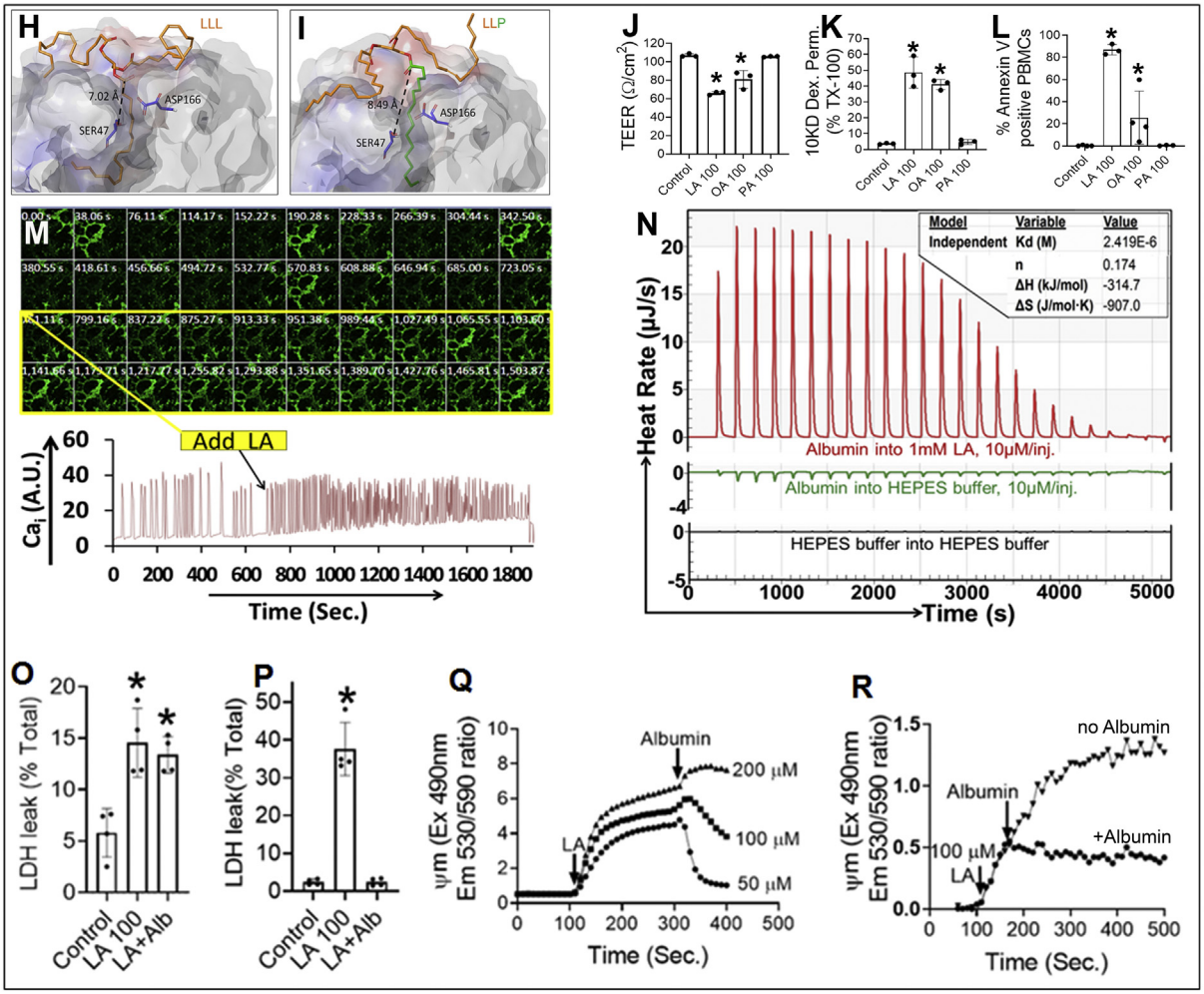

normal through COVID-19 is a low-cost, low-risk strategy to improve outcomes.

Supplementary Material

Note: To access the supplementary material accompanying this article, visit the online version of *Gastroenterology* at www.gastrojournal.org, and at https://doi.org/10.1053/j.gastro.2020.05.057.

References

1. Zhou F, et al. Lancet 2020;395:1054–1062.
2. **de Oliveira C, Khatua B**, et al. J Clin Invest 2020;130:1931–1947.
3. Navina S, et al. Sci Transl Med 2011;3:107ra110.
4. Lighter J, et al. Clin Infect Dis 2020.
5. Barlass U, et al. Clin Transl Gastroenterol 2020;11(7):e00215. doi:10.14309/ctg.0000000000000215.
6. Cao M, et al. medRχiv 2020. 2020.03.04.20030395.
7. Khatua B, et al. J Clin Med 2020;9:263.
8. Liu F, et al. Clin Gastroenterol Hepatol 2020;18:2128–2130.e2.

Author names in bold designate shared co-first authorship.

Received April 27, 2020. Accepted May 18, 2020.

Correspondence
Address correspondence to: Vijay P. Singh, MD, Division of Gastroenterology and Hepatology, Mayo Clinic, Scottsdale, AZ 85259. e-mail: singh.vijay@mayo.edu; fax: (480) 301-7017.

Acknowledgments
Lipotoxicity in COVID-19 Study Group contributors: Bara El-Kurdi, Biswajit Khatua, Christopher Rood, Christine Snozek, Sergiy Kostenko, Shubham Trivedi, Clifford Folmes, Katherine Minter Dykhouse, Sumbal Babar, Yu-Hui Chang, Rahul Pannala, Rodrigo Cartin-Ceba, and Vijay P. Singh.

We are extremely thankful to Jill Lauritsen, Sheila Sandolo, and the staff at the Mayo Clinic Arizona Biospecimen repository and accession core for their help. We acknowledge the websites worldometers.info/coronavirus, the Johns Hopkins University Coronavirus resource center (https://coronavirus.jhu.edu/), Wikipedia.com, the World Bank website (https://data.worldbank.org/) and World Health Organization website (https://apps.who.int/gho/data/view.main.HS07v) and data publicly provided by www.ourworldindata.org/.

CRediT Authorship Contributions
Bara El-Kurdi, MD (Data curation: Equal; Investigation: Equal; Methodology: Equal; Writing – original draft: Equal); Biswajit Khatua, PhD (Data curation: Equal; Investigation: Equal; Methodology: Equal); Christopher Rood, BS (Data curation: Equal; Formal analysis: Equal; Methodology: Equal); Christine Snozek, PhD (Data acquisition -Equal, Methodology: Equal, Writing – subsequent draft: Equal); Rodrigo Cartin-Ceba, MD (Data curation: Equal; Funding acquisition: Equal; Investigation: Equal; Methodology: Equal; Project administration: Equal; Supervision: Equal; Writing – original draft: Supporting); Vijay P. Singh, M.D. (Conceptualization: Lead; Data curation: Lead; Formal analysis: Lead; Funding acquisition: Lead; Investigation: Lead; Methodology: Lead; Project administration: Lead; Resources: Lead; Supervision: Lead; Validation: Lead; Visualization: Lead; Writing – original draft: Lead); The Lipotoxicity in COVID-19 Study Group (Data curation: Equal; Formal analysis: Equal; Investigation).

Conflicts of interest
The authors disclose no conflicts.

Funding
This project was supported by the following: R01DK092460, R01DK119646 from the National Institute of Diabetes and Digestive and Kidney Diseases, PR151612 from the Department of Defense (to Vijay P. Singh), and intramural support from the Mayo Foundation. Intramural funding from the Center for Biomedical Discovery Science Award (to Vijay P. Singh and Clifford Folmes) and MEGA award (to Rodrigo Cartin-Ceba) also contributed to the project.

Figure 1. (*A*) Schematic summarizing the study's approach. (*B*) Time course starting at the day of admission or –4 days (which ever came first) leading to the event on day 0, which is the day of discharge, death, or ICU admission. The green lines show the trends of those who were discharged to home, and the red lines show those who were transferred to the ICU or died. The AM laboratory test results collected on the day of dismissal are shown as day 1 to allow comparison of the trend. The upper panel shows the lowest oxygen saturation measured on pulse oximetry (Sao_2) in those admitted to the ICU. Also shown are total serum calcium (*middle panel*), and serum albumin (*lower panel*). *Significant ($P < .05$) difference for the whole time course matched for each day when comparing red and green values on *t* test. ‡Significant difference from admission or day –4. (*C*) Relationship of peak unbound fatty acids in ICU patients vs the ratio of partial pressure of oxygen to the percentage of oxygen being delivered (P/F ratio). (*D*) Parameters in mice given LA (C18:2), or palmitic acid (C16:0) at the mentioned doses. *$P < .05$, **$P < .01$, ***$P < .001$, ****$P < .0001$ on 1-way analysis of variance compared to controls. There were 8 mice per group. The terminal deoxynucleotidyl transferase–mediated deoxyuridine triphosphate nick-end labeling staining was done on paraffin sections of the spleen, and the percentage of positive cells in the white pulp was quantified. A drop in carotid artery distention supports hypotension and, when extreme, shock. Mice in the control and C16:0 groups were electively killed at 72 hours. (*E*) Univariate analysis of risk factors to percent mortality from COVID-19: each row mentions the parameter analyzed on the extreme left. The columns show the rate ratios, along with the 95% confidence intervals and *P* values for all countries with >1000 COVID cases reported between March 25, 2020, and April 8, 2020. (*F*, *G*) Graphical presentation (marginal plots) of countries showing the association between percent mortality from COVID-19 and (*F*) percent dietary unsaturated fat intake and (*G*) dietary saturated fat intake. The blue line is the expected value of the mortality change with respect to the value of saturated fat or percent UFA. The dots are the daily data. (*H*, *I*) Images of the induced-fit docking simulations of the (*H*) LA (C18:2) triglyceride of LLL and (*I*) 1,2-dilinoleoyl-3-palmitoyl-rac-glycerol (LLP) docked into the catalytic pocket (*dark gray*) of ATGL by using Schrodinger Maestro. The dashed line shows the distance of the triglyceride's primary carbonyl group in angstroms from the catalytic serine (SER47). (*J*, *K*) Bar graphs with standard deviation from HUV-EC-C cell monolayers exposed for 2 hours to 100 μmol/L of the fatty acid below the respective bar showing (*J*) transendothelial cell electrical resistance and (*K*) leakage of 10-kD dextran from the upper chamber into the lower chamber. The leakage induced by 1% Triton-X 100 was taken as 100%. *$P < .05$ vs control in *t* test. Each point for a condition represents a separate experiment. (*L*) Percentage of peripheral blood mononuclear cells staining positive for Annexin V after a 60-minute treatment with 100 μmol/L of the fatty acid below the respective bar. (*M*) Time series (images *above*, graph *below*), of Fluo-4AM-loaded cardiomyocytes showing the change in florescence signal after the addition of 150 μmol/L LA (C18:2; *yellow rectangle* in images). (*N*) Representative thermograms showing the heat rate of albumin interacting with C18:2 (*red lines*) with thermodynamic parameters in the inset box. Also shown are thermograms of albumin injection into HEPES buffer (*green line*) and buffer injection into buffer (*black line*). (*O*) The effect of adding 160 μmol/L albumin 30 minutes after adding 100 μmol/L LA on lactate dehydrogenase (LDH) leakage from J774 A.1 cells. (*P*) The effect of preincubating HEK293 cells with 160 μmol/L albumin and 2 mmol/L calcium (LA + Alb) on 100 μmol/L LA-induced injury (LA 100). (*Q*, *R*) Representative curves showing the effect of adding 160 μmol/L albumin 300 seconds (*Q*) after inducing ψm by different concentrations of LA in HEK293 cells or (*R*) after 150 seconds in pancreatic acinar cells. CI, confidence interval; Em, emission; Ex, excitation; ICU, intensive care unit; M, mol/L; OA, oleic acid; PA, palmitic acid; PBMC, peripheral blood mononuclear cells; Sec., seconds; TEER, transendothelial cell electrical resistance.

Supplementary Data

Human Data

Protocols (14-003999, 18-005104) were approved by the Mayo Clinic institutional review board (IRB). Chart review of patients admitted with COVID-19 infection from March 20, 2020, and April 7, 2020 was done (by VPS and RCC). More than 1 admission over a 2-week period was counted as 1. Data were collated into an Excel spreadsheet (Microsoft, Redmond, WA), graphed, and statistically compared. Unbound fatty acids were measured on residual serum samples remaining after all clinical testing was done, as per the approved IRB protocol. All consenting requirements stipulated by the approved IRB protocol were followed.

Epidemiologic Data

Real-time database searches between March 25, 2020, and April 8, 2020, were done. Total COVID-19 cases and deaths (www.worldometers.info/coronavirus) were validated from (https://coronavirus.jhu.edu/) for all countries, with a total of >1000 cases. All countries reporting >20 deaths were included until day 7. A country's area, population (in millions), gross domestic product (GDP) (in billions of US dollars), latitude, hospital beds/1000 population, and ICU beds/100,000 population were from Wikipedia and were validated from https://data.worldbank.org/, https://apps.who.int/gho/data/view.main.HS07v, and www.ourworldindata.org/. The calculated parameters were "% deaths," "COVID positive/million," "population density," and "per capita GDP."

The per capita (kg/capita/year) food intake of each country was recorded from http://www.fao.org/faostat/en/#data/FBS, by choosing "country," and then "Element" as "food supply quantity (kg/capita/year)". Under "items aggregated," "Animal products (list)" and "vegetable oils (list)" were chosen, as was year "2017". Data were downloaded as a .csv file and converted to Excel. Cold-source (unsaturated) fat intake (kg/capita/year) was as total vegetable oil intake (excluding palm oil) + fish fat (10% of weight of fish consumed). The warm-source fat (saturated) intake (kg/capita/year) was palm oil + ghee + butter + cream + raw animal fat + 15% of red meat and mutton weight + 8% of pork weight + 14% of poultry weight + 2% of milk weight. The percent cold-source (ie, unsaturated) fat was calculated as a percentage of cold + warm sources. National life expectancy, median age, and infant mortality were from https://www.un.org/development/desa/publications/publication, and COVID-19 doubling time were from www.ourworldindata.org/.

Statistics

The univariate analysis was performed by fitting a linear mixed model to evaluate the relationship between daily mortality and each variable, with a random intercept for each country to account for the clustering effect. The logarithm transformation estimates reflect the differences in the log of mortality rate per 1-unit increase in each explanatory variable. To quantify the association in the original scale of mortality rate, we exponentiated the model estimate, and hence, the value represents the rate ratio per 1-unit increase in an explanatory variable. A rate ratio of <1 indicates that an explanatory variable is negatively associated with mortality, a rate ratio of >1 indicates a positive association, and a ratio equal to 1 indicates no statistical association. The analysis was conducted based on the aggregated information from countries with available data. The statistical analysis was performed by the use of R 3.6.2 (R Project for Statistical Computing, Vienna, Austria).

Animal Experiments

Male, 8–10-week-old Institute for Cancer Research (ICR) mice (Charles River Laboratories, Wilmington, MA) were used as previously described.[1] There were 4 groups: control and intraperitoneal C18:2,[2] C18:1,[1] and C16:0 at 0.2%, 0.3%, and 0.5% body weight, respectively. These cohorts overlapped with but were not identical to the previous ones. All protocols were approved by the Institutional Animal Care and Use Committee of the Mayo Clinic Foundation.

Reagents

All reagents, including dimethyl sulfoxide (DMSO), were from Sigma-Aldrich (St Louis, MO).

Lipid Studies

As previously reported,[2] fatty acids were sonicated into phosphate-buffered saline (10 s/pulse × 3). C16:0 (insoluble in phosphate-buffered saline) was a 60-mmol/L stock in DMSO. Final DMSO (0.16%–0.5%) does not affect results, as shown previously.[4]

In Vitro Cell Studies

All data shown are from a 3–5 independent experiments.

Cell Lines and Cell Culture

Primary pancreatic acini peripheral blood mononuclear cells were harvested and used as described previously[5,6] in HEPES buffer pH 7.4 (20 mmol/L HEPES, 120 mmol/L NaCl, 5 mmol/L KCl, 1 mmol/L $MgCl_2$, 10 mmol/L glucose, 10 mmol/L sodium pyruvate, 1 mmol/L $CaCl_2$), as were HEK293 cells.[2] J774A.1 cells cultured as per American Type Culture Collection (Manassas, VA) were gently scraped, washed 3 times in HEPES buffer at 37°C, exposed to LA for 2 hours (75 revolutions/minute). LDH leakage was calculated as for HEK293 cells. Human endothelial cell Established human umbilical vein endothelial cell (HUV-EC-C) monolayers (on 0.4-μm polyester Transwell permeable membrane [Corning, NY] precoated with type IV collagen) were grown in Kaighn's modification of Ham's F-12 medium, and supplemented with 10% fetal bovine serum, 1% penicillin/streptomycin, 0.1 mg/mL heparin, and 50 μg/mL Corning Endothelial Cell Growth Supplement, as per American Type Culture Collection. TEER measurement (in Ωcm^2) using the EVOM2 Epithelial Volt/Ohm Meter with an STX2 electrode (World

Precision Instruments, Sarasota, FL) and 10-kD dextran Alexa Fluor 647 permeability tracer flux assay (added to the upper chamber, measured in the lower chamber) were done in HEPES buffer over 2 hours of non-esterifed fatty acid (NEFA) treatment.

Mitochondrial Depolarization Studies

Mitochondrial depolarization (ψm) studies were done as described previously.[4,7–9]

Unbound Fatty Acids

Unbound fatty acids were measured following manufacturer's protocol for the ADIFAB2 kit (FFA Sciences, San Diego, CA). Readings were calibrated against NEFA standards made in DMSO.

Albumin-C18:2 Binding

This was done by using isothermal titration calorimetry at 37°C as recently described[2] by using 850-μmol/L fatty acid–free bovine serum albumin in the burette, with 10 μmol/L/injection into 1 mmol/L C18:2.

Molecular Docking

The crystal structure of human ATGL has yet to be elucidated, which necessitated the construction of an ATGL homology model with SWISS-MODEL[10] to perform molecular docking simulations. Triglycerides trilinolein; LLL (compound CID: 5322095), 1,2-dilinoleoyl-3-palmitoyl-rac-glycerol; LLP (compound CID: 9544106), 1-linoleoyl-2-oleoyl-3-palmitoyl-sn-glycerol; and LOP (compound CID: 99647498) were docked to the ATGL homology model using the Induced Fit Docking protocol within Schrodinger Maestro.[11]

Human Induced Pluripotent Stem Cell–Derived Cardiomyocytes

Cardiomyocytes were generated from human induced pluripotent stem cells (IRB 13-007298 and 18-010099) by using the chemically defined medium 3 (CMD3) protocol[12] with modifications.[13] Briefly, induction of differentiation was achieved by using 8 μmol/L CHIR-99021 and 10 nmol/L activin A for 20 hours, followed by treatment with 5 μmol/L IWP2 and 10 ng/mL of recombinant human BMP-4. Cardiomyocytes were not subject to lactate selection before dissociation on day 15 and were seeded on fibronectin-coated, glass-bottomed plates for imaging. These were loaded with Fluo-4AM and imaged[14] (Zeiss LSM 800; Carl Zeiss, Oberkochen, Germany) in HEPES buffer/37°C/every 9.5 seconds ± LA. Fluorescence (arbitrary units) was quantified on fixed areas of serial images using ImageJ software (National Institutes of Health, Bethesda, MD).

Supplementary References

1. de Oliveira C, Khatua B, Noel P, et al. Pancreatic triglyceride lipase mediates lipotoxic systemic inflammation. J Clin Invest 2020;130:1931–1947.
2. Khatua B, Yaron JR, El-Kurdi B, et al. Ringer's lactate prevents early organ failure by providing extracellular calcium. J Clin Med 2020;9(1):263.
3. Khatua B, Trivedi RN, Noel P, et al. Carboxyl ester lipase may not mediate lipotoxic injury during severe acute pancreatitis. Am J Pathol 2019;189:1226–1240.
4. Navina S, Acharya C, DeLany JP, et al. Lipotoxicity causes multisystem organ failure and exacerbates acute pancreatitis in obesity. Sci Transl Med 2011; 3(107):107ra110.
5. Noel P, Patel K, Durgampudi C, et al. Peripancreatic fat necrosis worsens acute pancreatitis independent of pancreatic necrosis via unsaturated fatty acids increased in human pancreatic necrosis collections. Gut 2016; 65:100–111.
6. Patel K, Trivedi RN, Durgampudi C, et al. Lipolysis of visceral adipocyte triglyceride by pancreatic lipases converts mild acute pancreatitis to severe pancreatitis independent of necrosis and inflammation. Am J Pathol 2015;185:808–819.
7. Singh VP, Bren GD, Algeciras-Schimnich A, et al. Nelfinavir/ritonavir reduces acinar injury but not inflammation during mouse caerulein pancreatitis. Am J Physiol Gastrointest Liver Physiol 2009;296:G1040–G1046.
8. Singh VP, McNiven MA. Src-mediated cortactin phosphorylation regulates actin localization and injurious blebbing in acinar cells. Mol Biol Cell 2008;19:2339–2347.
9. Patel K, Durgampudi C, Noel P, et al. Fatty acid ethyl esters are less toxic than their parent fatty acids generated during acute pancreatitis. Am J Pathol 2016; 186:874–884.
10. Waterhouse A, Bertoni M, Bienert S, et al. SWISS-MODEL: homology modelling of protein structures and complexes. Nucleic Acids Res 2018;46(W1):W296–W303.
11. Schrödinger. Glide release 2020-1: induced fit docking protocol: prime. New York: Schrödinger, 2020.
12. Burridge PW, Holmstrom A, Wu JC. Chemically defined culture and cardiomyocyte differentiation of human pluripotent stem cells. Curr Protoc Hum Genet 2015; 87(1):21.3.1–21.3.15.
13. Perales-Clemente E, Cook AN, Evans JM, et al. Natural underlying mtDNA heteroplasmy as a potential source of intra-person hiPSC variability. EMBO J 2016; 35:1979–1990.
14. Muili KA, Wang D, Orabi AI, et al. Bile acids induce pancreatic acinar cell injury and pancreatitis by activating calcineurin. J Biol Chem 2013;288:570–580.

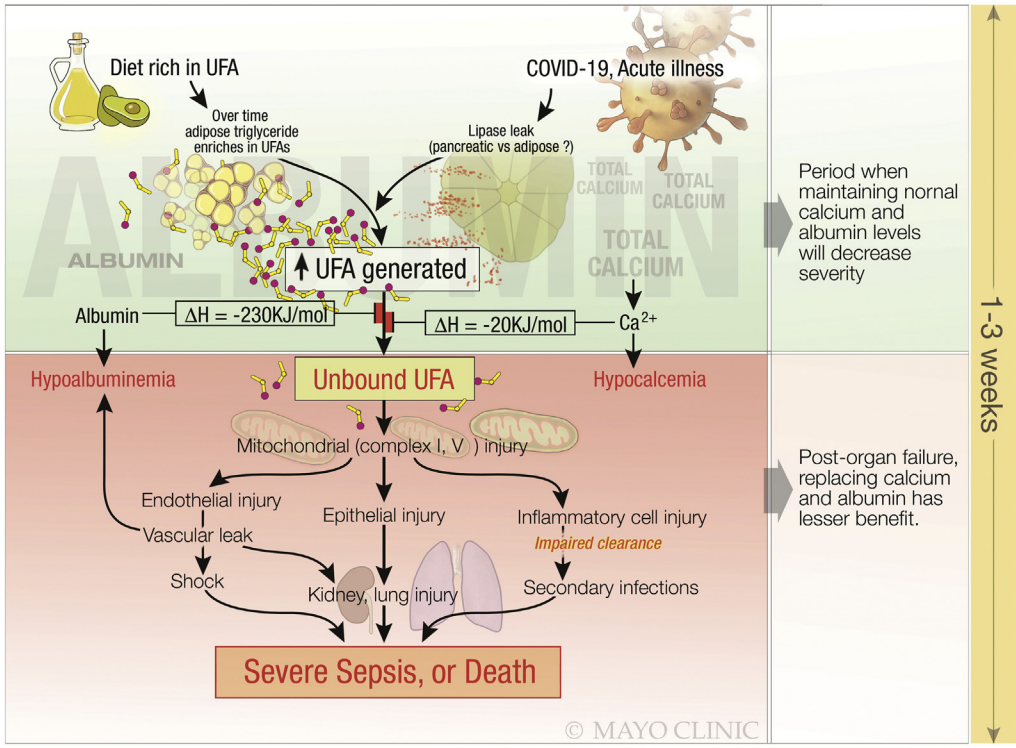

Supplementary Figure 1. Schematic describing how a diet rich in unsaturated fat, makes adipocyte triglyceride unsaturated, which predisposes to severe COVID-19, resulting in severe sepsis or death, and how this can be prevented earlier in the disease. The early phase of the disease (green background) is before organ failure has set in. At this time neutralization of the UFAs by albumin and calcium can reduce toxicity from the unbound form of UFAs. However, once the UFAs have cause mitochondrial complex I and V to be injured in the multiple vital cell types (red background), organ failure sets in. At this time supplementing albumin and/ or calcium is ineffective, since the fatty acids have already caused mitochondrial damage and organ failure. Therefore early supplementation of calcium and albumin may prevent the progression of COVID-19 to a severe disease.

A

	Discharged	ICU/died	*P*
Number	7	7	NS
Age (Yr. ± SD)	62.9±14.6	63.4±11.3	NS
Sex (M:F)	5 : 2	2 : 5	NS
BMI ± SD	31.1± 3.8	28±4.6	NS
hypertension	3	3	NS
Hyperlipidemia	4	3	NS
Type-2 Diabetes	1	3	NS
COPD	0	1	NS
Asthma	2	0	NS
Obstructive sleep apnea	1	2	NS
Chronic kidney disease	0	1	NS
Atrial fibrillation	0	1	NS
Previous History of			
Low grade neoplasm	1	2	NS
Transplant	0	1	NS
Pneumonia	1	0	NS
Neuro degn. disease	0	1	NS

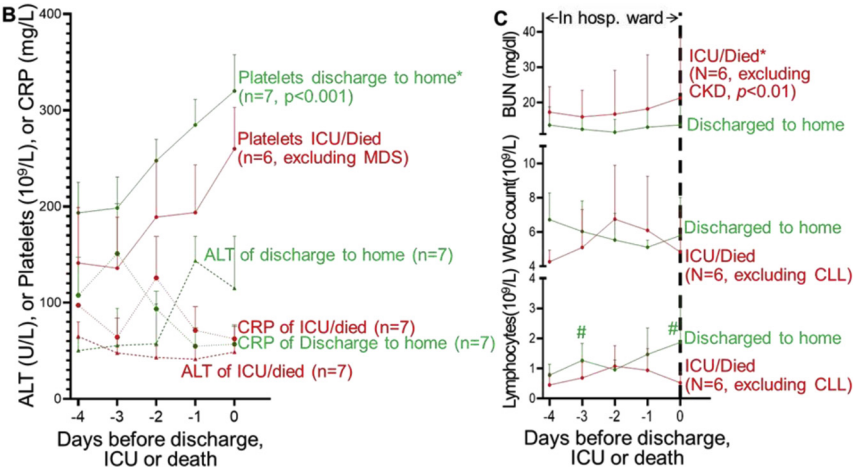

Supplementary Figure 2. (*A*) Table comparing the demographics and comorbidities of patients with COVID-19 who were discharged home vs those who were admitted to the ICU or died (ICU/died). (*B*) Time course starting at the day of admission or –4 days (whichever came first) leading to the event on day 0, which is the day of discharge; death; or ICU admission. The green lines show the trends of those who were discharged to home, and the red lines show those who were transferred to the ICU or died. From top to bottom, these are morning (AM) laboratory values for platelet counts, serum alanine aminotransferase, and C -reactive protein. *Significant ($P < .05$) difference for the whole time course matched for each day when comparing red and green values on *t* test. One patient who died had myelodysplastic syndrome and was excluded. (*C*) The patterns for BUN, total WBC counts, and absolute lymphocyte counts. The patients excluded are mentioned, along with the underlying comorbidity. #Significant difference between red and green values for the day. ALT, alanine aminotransferase; BMI, body mass index; BUN, blood urea nitrogen; CKD, chronic kidney disease; CLL, chronic lymphocytic leukemia; CRP, C-reactive protein; COPD, chronic obstructive pulmonary disease; degn., degenerative; F, female; hosp., hospital; M, male; SD, standard deviation; WBC, white blood cell; Yr., years.

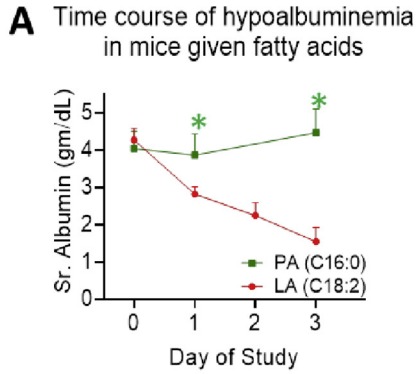

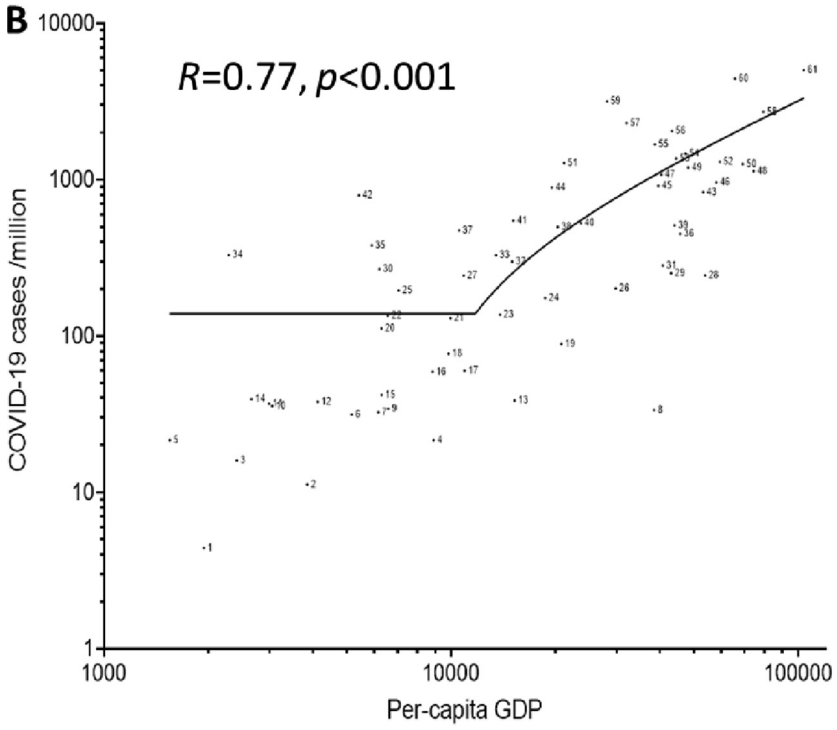

Country No.	Country	Country No.	Country
1	india	31	UAE
2	indonesia	32	Chile
3	Egypt	33	Croatia
4	Mexico	34	Moldova
5	Pakistan	35	Serbia
6	iraq	36	Finland
7	South Africa	37	Turkey
8	Japan	38	Czechia
9	Thailand	39	Canada
10	Morocco	40	Slovenia
11	phlippines	41	Panama
12	Algeria	42	Iran
13	Argentina	43	Sweden
14	Ukraine	44	Estonia
15	Colombia	45	UK
16	China	46	Denmark
17	Russia	47	Israel
18	Brazil	48	Norway
19	Saudi Arabia	49	Netherlands
20	Belarus	50	Ireland
21	Malaysia	51	Portugal
22	Peru	52	USA
23	Poland	53	Germany
24	Greece	54	Austria
25	Dominican Republic	55	France
26	S. Korea	56	Belgium
27	Romania	57	Italy
28	Australia	58	Switzerland
29	New Zealand	59	Spain
30	Ecuador	60	Iceland
		61	Luxembourgh

Data from 61 countries with > 1000 COVID-19 cases (total 1476418) on 4-8-2020

Supplementary Figure 3. (*A*) Time course of serum albumin levels in mice given the UFA LA (C18:2, *red line*) vs those give palmitic acid (C16:0, *green line*). There were 8 mice per group. *$P < .0001$ vs for same-day values measured in the 2 groups of mice. (*B*) Nonlinear correlation of the number of COVID-19 cases diagnosed/million population of a country and its per capita GDP as of April 8, 2020, which was the last day of the study. Note that the inflection point for increase in testing is noted at approximately US$15,000. The table on the right gives the name of the country corresponding to the number shown. PA, palmitic acid; Sr., serum; UAE, United Arab Emirates.